Synthesis and Magnetic Properties of Double Perovskite La_2BMnO_6 (B = Ni or Co) Nanoparticles

Y. Mao[*], J. G. Parsons[*], and J.S. McCloy[**]

[*]Department of Chemistry, University of Texas - Pan American, Edinburg, TX 78539 USA, maoy@utpa.edu

[**]Energy & Environment Directorate, Pacific Northwest National Laboratory, Richland, WA 99352 USA, john.mccloy@pnnl.gov

ABSTRACT

Double perovskite La_2BMnO_6 (B = Ni and Co) nanoparticles with average particle size of ~50 nm were synthesized using a facile, environmentally friendly, scalable molten-salt reaction at 700 °C in air. Their structural and morphological properties were characterized by x-ray diffraction and transmission electron microscopy. Their magnetic properties were evaluated using dc magnetic *M-T* and *M-H*, and ac magnetic susceptibility versus frequency, temperature, and field for the first time. The dc magnetization curves show paramagnetic-ferromagnetic transitions at T_C ~275 and 220 K for La_2NiMnO_6 (LNMO) and La_2CoMnO_6 (LCMO) nanoparticles, respectively. ac susceptibility revealed that the LCMO nanoparticles had a single magnetic transition indicative of Co^{2+}-O^{2-}-Mn^{4+} ordering, whereas the LNMO nanoparticles showed more complex magnetic behaviors suggesting a re-entrant spin glass.

Keywords: core@shell; energy storage; manganese oxide; nanoforest; three-dimensional

INTRODUCTION

Double perovskite oxides with a general formula $AA'BB'O_6$ (where A and A' are rare earth or alkaline earth metals, and B and B' are *d*-block transition metals) display a wide variety of interesting physical properties with composition variations. Considerable research is being carried out to explore new double perovskite materials, to understand the origin of their properties (e.g. magnetodielectric, magnetoresistance, and magneto-capacitance), to improve their properties, and to adapt their materials chemistry to production technology for each application.[1] The studies are primarily driven by advances in the synthetic and characterization techniques of complex compositions and structures and motivated by the demands for higher-density information recording media, spintronics, magnetic field sensors, and infrared detectors, among many other applications.[1a, 1b, 2]

One of the double perovskite oxides, La_2NiMnO_6 (LNMO) has gained more attention as a rare example of a single-material platform with multiple functions, such as ferromagnetic (FM) insulating properties up to room temperature, magnetocapacitance, and magnetoresistance effects.[1a, 3] Due to its spin lattice coupling which results in a large magnetodielectric (MD) effect close to RT, it has been demonstrated that the spins, electric charge and dielectric functions in LNMO can be tuned by magnetic or electric fields.[1a-f] It has also been confirmed that LNMO is a FM semiconductor that has a Curie temperature (T_C) very close to RT, with ordered Ni^{2+} and Mn^{4+} ions occupying the centers of corner-sharing BO_6 and $B'O_6$ in the structure, respectively, thus distorting the ideal double perovskite. This conclusion is consistent with the Mn NMR and x-ray absorption spectroscopic results on LNMO powders.[4] In some neutron and x-ray diffraction studies, bulk LNMO provided evidence for long-range ordering of Ni and Mn cations, even though different neutron-diffraction studies disagree on whether the oxidation states are Ni^{2+}/Mn^{4+} or Ni^{3+}/Mn^{3+}.[1a, 5]

LNMO's isostructural system, La_2CoMnO_6 (LCMO), possesses a FM T_C ~225 K with an insulating behavior.[1c, 1g] Similar to those of the LNMO system, several reports have also shown that the magnetic properties of the LCMO system are strongly related to cation ordering (especially arrangement of B-site ions), cation valences, and defects, all of which depend significantly on the synthesis conditions.[1c, 1g, 3a, 6] For instance, LNMO and LCMO can exhibit one or more magnetic transitions. LNMO synthesized under some conditions shows two unobscured FM transitions occurring at ~280 K and~150 K as measured by decreasing temperature.[1c, 7] An ordered sublattice with high spin Co^{2+} and Mn^{4+} pairs in LCMO gives a FM transition at ~220 K, while a disordered sublattice with low spin Co^{3+} and high spin Mn^{3+} results in a FM transition below 150 K.[1c] It was also reported that in the case of low temperature sintered LCMO samples, high T_C (~220 K) was observed while the samples prepared at high temperature exhibited low T_C (~150 K).[6d] In ordered LCMO thin films, observed MD effect near T_C was attributed to spin-lattice coupling. On the other hand, only 0.8% of MD response was observed at 280 K in polycrystalline LCMO.[8] Raman measurements showed a spin-lattice coupling near the two magnetic transitions in bulk LCMO.[6a]

The mechanisms determining ferromagnetism in manganites include double exchange (DE) and superexchange (SE). SE-like interactions may yield FM insulating (FMI) or antiferromagnetic(AFM) phases.[9] The

FM SE interaction between B-site and Mn ions through oxygen in La_2BMnO_6 has been employed to explain the large influence of synthesis conditions on magnetic properties.[8] Two more cases exist: AFM interactions between half-filled orbitals and FM interactions between half-filled and empty or full orbitals. For double perovskite manganites, La_2BMnO_6, it is well-known that anti-site disorder with an interchange between B and Mn sites also has profound effects on physical properties, especially magnetic properties.[1e, 1g, 8]

Recently, nanostructures have been investigated as emerging materials because they exhibit interesting chemical and physical properties which are different from those of their bulk and thin film counterparts.[10] For manganites, such as LNMO and LCMO, when their particle size is reduced to the nanometer scale, the possible new mechanisms include superparamagnetic (SPM), superferromagnetic (SFM), and spin-glass (SG) behaviors due to different interparticle magnetic interactions ranging from weakly to strongly interacting.

In the case of double perovskite manganites, the majority of the previous work has focused on $AA'BB'O_6$ single crystals and thin films. However, it can be concluded that the discrepancies mentioned above from the studies of both LNMO and LCMO samples are originated from the different synthetic procedures and conditions employed. So far, there are very few reports on LNMO and LCMO nanostructures. To the best of our knowledge, there is no reported comparison yet on the magnetic properties of LNMO and LCMO nanostructures. In the current work, we investigated magnetic properties of LNMO and LCMO nanoparticles prepared by a facile and scalable molten-salt synthesis process.[11, 12] More importantly, we investigated here not only field-cooled and zero-field-cooled magnetization and magnetic field dependences of magnetization of these nanoparticles, but also their alternating current (ac) susceptibilities. ac susceptibility was used as a powerful tool to study the magnetic properties in our as-synthesized LNMO and LCMO nanoparticles, as it has been for the study of other manganite and related systems, such as $Pr_{0.7}Ca_{0.3}MnO_3$,[13] $La_{0.7}Ca_{0.3}MnO_3$,[14] $La_{0.5}Sr_{0.5}CoO_3$,[15] $La_{0.8}Sr_{0.2}(Mn_{0.925}Ti_{0.075})O_3$,[16] and $Ca_2Fe_{0.8}Co_{0.2}MoO_6$.[17]

RESULTS AND DISCUSSION

Powder XRD was used to characterize the as-synthesized LNMO and LCMO nanoparticles. No extra reflection peaks other than those of pure perovskite phase are observed within the experimental limit, which confirms the formation of single phase composition of LNMO and LCMO double perovskites (data not shown).[1b, 5, 18, 19]

Figure 1 shows general TEM images of LNMO and LCMO nanoparticles. These images demonstrated that LNMO and LCMO nanoparticles with particle sizes of 65 ± 18 nm and 58 ± 20 nm (based on 45 particles each), respectively, are prepared by the molten-salt synthetic procedure at temperature of 700 °C.

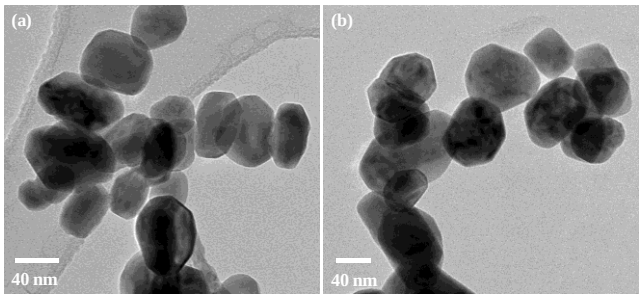

Figure 1 Typical TEM images of the as-synthesized (a) LNMO and (b) LCMO nanoparticles.

The temperature dependence of zero-field-cooled (ZFCW) and field-cooled (FCC) dc magnetization of the as-synthesized LNMO nanoparticles was measured (Figure 2a). The onset of magnetization indicates a Curie transition temperature of ~275 K due to FM long-range ordering, very close to the magnetic transition temperature (T_C = 280 K) reported previously in the literature for the bulk material and in the range reported for other LNMO materials.[1a-f, 18b] This transition temperature is also characteristic of atomically ordered Ni^{2+} and Mn^{4+}ions. Small differences in T_C may be attributed to the finite size scaling and/or the surface strain effects of these nanoparticles.[3b] Additionally, the *M-T* curves also show minor discontinuities at ~175 K and ~90 K (Figure 2a, upper inset). Both low temperature anomalies have been reported previously for rhombohedral LNMO powder prepared at lower temperature by the Pechini processing method, rather than the traditional solid-state reaction, but these features were not assigned.[18a, 18b]

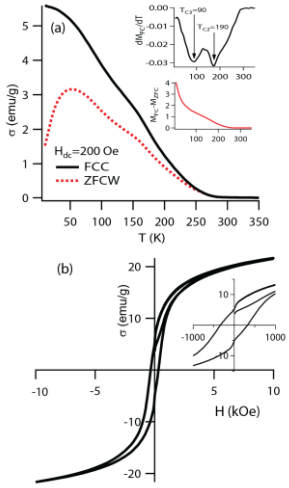

Figure 2 LNMO nanoparticles: (a) Temperature dependence of ZFC and FC magnetization in an applied field of 200 Oe. The insets shows the plot of dM_{FC}/dT as a function of temperature at H = 200 Oe and the difference M_{FC}-M_{ZFC}. (b) Field-dependent magnetization data at 10 K up to ±10 kOe. The inset shows a magnified view near zero field.

Figure 2b shows the *M-H* curves of LNMO nanoparticles, showing a hysteresis loop at 10 K with a coercive field ~500 Oe and remnant magnetization ~6 emu/g. At temperature higher than T_C (T > 280 K), the *M-H* behavior is linear, corresponding to a paramagnetic state (not shown). In these LNMO nanoparticles the saturation moment is much smaller than most LNMO previously measured from powders and thin films, and is closest to, but still smaller than, the LNMO samples with ~20% known anti-site defects.[18b] It cannot be

ruled out that these nanoparticles exhibit some fraction of SPM sites, some surface disorder, and/or large fractions of anti-site disorder which result in the low specific saturation magnetization.

Figure 3 shows that our LNMO nanoparticles display frequency dependence of ac susceptibility. The point at which $\chi'(T)$ and $\chi''(T)$ approach zero is ~275 K, corresponding to T_C, as in the dc measurements (Figure 2a). As shown in Figure 3a, the χ' decreases in intensity with increasing frequency. And the shape of χ' is very similar to the ZFC dc magnetization measured under low field (Figure 3a), as has been observed previously with similar systems, such as $Ca_2Fe_{1-x}Co_xMoO_6$ ($0.1 \leq x \leq 0.4$).[17] The χ'' is more revealing (Figures 3c and 3d), showing clear peaks T_{f1} at ~175 K and T_{f2} at ~65 K for 10 kHz. The T_{f1} peak is not frequency (f) dependent while the T_{f2} peak is, with higher frequencies moving the peak to higher temperatures in a manner suggesting a disordered state similar to a spin glass. Hence, the LNMO nanoparticles exhibit successive transitions from paramagnetic to ferromagnetic to spin glass as temperature is decreased, thereby being classed as a re-entrant spin glass (RSG).[16-17, 21] At present, the possibility cannot be ruled out that the two distinctly different magnetic phases (i.e., one containing Mn^{3+} and Ni^{3+} and the other containing the expected Mn^{4+} and Ni^{2+}) in our nanostructured sample originate from an inhomogeneous sample. The asymmetrical peak T_{f1} in χ'' ~175 K in our data is less easily explained, and may consist of multiple unresolved peaks, one at 150 K suggesting a second phase with different cation valences.[7] On the other hand, Iliev et al.[22] have suggested that a feature at 188 K in their LNMO samples is due to short range Ni/Mn ordering in a fraction of the sample. One clear change in T_{f1} is that it is suppressed with the application of an external dc field, resulting in a reduction of χ' (Figure 3b) and drastic reduction of χ'' near T_{f1} (Figure 3d). The exact mechanisms responsible for this observation are as yet unresolved.

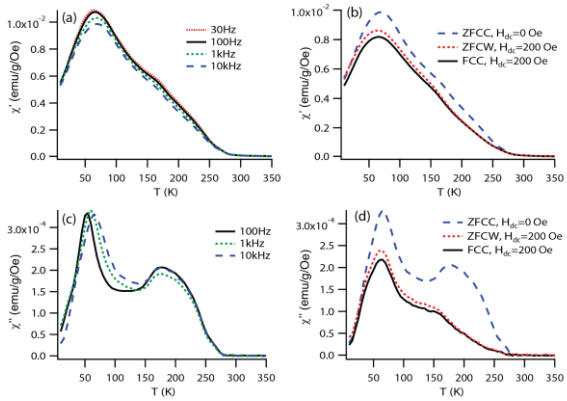

Figure 3 LNMO nanoparticles: Temperature dependence of (a,b) real component (χ') and (c,d) imaginary component (χ'') of ac magnetic susceptibility. (a,c) At zero dc field-cooled cool-down (ZFCC, H_{dc} = 0) as a function of frequency. (b, d) At 10 kHz as a function of heating/cooling direction and field.

The temperature dependence of ZFCW and FCC dc magnetization was also measured for the as-synthesized LCMO nanoparticles from 10 to 350 K in a 200 Oe magnetic field (Figure 4a). Below 210 K, ZFC and FC magnetization curves diverge, similarly to the data measured from LNMO nanoparticles. These LCMO nanoparticles possess a single magnetic transition ~235 K under 200 Oe field, which is very close to the magnetic transition temperature reported previously for the well-ordered bulk LCMO.[1g]

Figure 4b shows the M-H curves of LCMO nanoparticles. At temperature higher than T_C (T > 210 K), the M-H behavior is linear (not shown), corresponding to a paramagnetic state. A hysteresis loop has been observed at 10 K, with a coercive field of ~8.5 kOe and a remnant magnetization of ~20 emu/g. The saturation magnetization of M_S ~ 3.67 μ_B/f.u (obtained from 70 kOe data point) is substantially less than the theoretically calculated spin only value of 5.89 μ_B/f.u. It can be seen that the moment lies well within the range of previously reported LCMO materials, particularly those from Dass and Goodenough.[1c] The jog in magnetization (Figure 4b) at zero field has also been observed previously in LCMO.[6e] This so-called "bi-loop" is often indicative of two magnetic phases with different coercive fields,[6e, 23] but in the case of LCMO it has been argued that the bi-loop results from magnetic domains of the same crystal structure and chemistry but with slightly different lattice parameters due to tilting of the MnO_6 and CoO_6 octahedra.[1g, 6c] It should be noted that the LNMO exhibits this bi-loop feature as well in the M-H curve, though less dramatically (Figure 2b inset), and this bi-loop been observed also in another double perovskite, Ca_2FeReO_6, as well.[24]

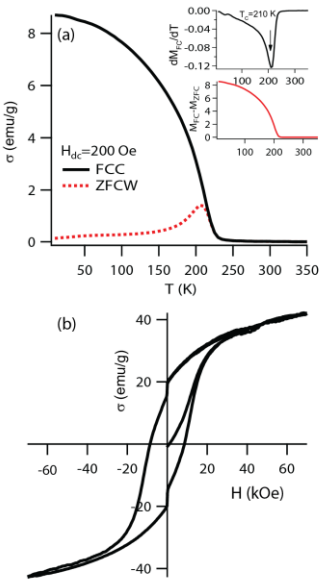

Figure 4 LCMO nanoparticles: (a) Temperature dependence of ZFC and FC magnetization in an applied field of 200 Oe. The insets show the plot of dM_{FC}/dT as a function of temperature at H = 200 Oe and the difference M_{FC}-M_{ZFC}. (b) Field-dependent magnetization data at 10 K up to ±70 kOe.

The LCMO nanoparticles measured in the ZFCC condition show frequency dependence of ac susceptibility, in both real component (χ') and imaginary components (χ'') (Figures 5a and 5c, respectively), though of a much different character than that observed for the LNMO

nanoparticles (Figure 3). Only one peak is evident (~210 K, which is very close to the peak of the M_{ZFC} curve at ~205 K shown in Figure 4a), and the real and imaginary parts of the ac susceptibility are very similar. The peak decreases in intensity with increasing frequency, more dramatically for χ' than for χ", but the peak frequency appears temperature independent. Note that this result is different than that of Wang et al[25] who showed a slight peak frequency dependence of the ~210 K peak when measuring at 1 K increments (finer scale than our 5 K increments). Figures 5b and 5d show the variation of ac susceptibility at 10 kHz depending on heating/cooling and application of an external dc field, showing that zero field-cooled cool-down (ZFCC) with no applied field gives the largest ac signal with a peak at 215 K (χ' and χ"), but the peak shifts to the lower temperature 210 K (χ') or 205 K (χ"), with applied field of 200 Oe, either with zero field-cooled warm-up (ZFCW) or field-cooled cool-down (FCC). Unlike for LNMO, the ZFCW and FCC curves are indistinguishable in the LCMO particles. The frequency independence of the peak, and the damping with applied external dc field both suggest that the peak can be assigned to the Hopkinson effect, in which the susceptibility reaches a maximum just below T_C due to the vanishing of the anisotropy at and above T_C.[14, 26]

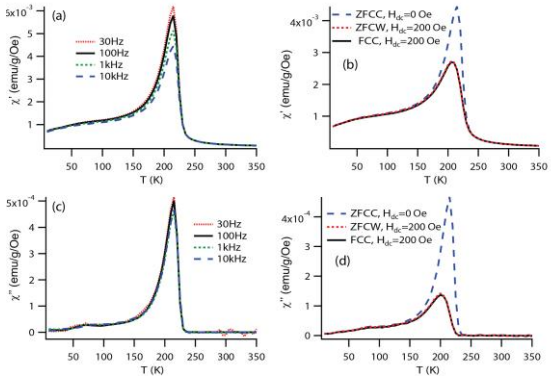

Figure 5 LCMO nanoparticles: Temperature dependence of (a,b) real component (χ') and (c,d) imaginary component (χ") of ac magnetic susceptibility. (a,c) At zero dc field-cooled cool-down (ZFCC, H_{dc} = 0) as a function of frequency. (b, d) At 10 kHz as a function of heating/cooling direction and field.

In these curves, the cusps at T_C ~205-215 K can be assigned to a strong PM-FM phase transition, attributed to the FM superexchange interactions of the ordered Co^{2+}-O^{2-}-Mn^{4+} pair.[1c, 6a, 27] No weak FM transition at T_C ~135-150 K was observed as reported previously on bulk and thin film samples of LCMO, usually assigned to FM vibronic superexchange interaction of intermediate spin Co^{3+} ($t_{2g}^5 e_g^1$)-high spin Mn^{3+} pair.[6c, 8] This peak results from occurrence of disordered phase and/or oxygen vacancies during the synthesis of LCMO samples. The 150 K peak has also been described as occurring only in the orthorhombic phase, whereas the rhombodehral phase exhibits only the ~225 K transition.[6d] Furthermore, our LCMO nanoparticles do not show a low temperature transitions at ~ 33-50 K, which indicate disordered Co^{3+}/Mn^{3+} regions with ordered Co^{2+}/Mn^{4+} regions.[8] Together these results suggest that there is no Co^{3+} in these LCMO nanoparticles, but rather they exhibit ordered Co^{2+}-O^{2-}-Mn^{4+} pairs.

CONCLUSIONS

In summary, nanoparticles with double perovskite structure, La_2BMnO_6 (B = Ni and Co) composition and an average size of ~50 nm have been successfully synthesized by a simple, scalable, and efficient molten salt synthetic process using metallic nitrates as precursors. The magnetic properties of these double perovskite nanoparticles indicate that they possess very different magnetic behaviors. The following results were obtained in the present investigation: (i) Field-cooled and zero-field-cooled magnetization curves become divergent at their Curie temperature, i.e. 275 K and 210 K for LNMO and LCMO nanoparticles, respectively, which are almost unchanged from their bulk and thin film counterparts. (ii) ac susceptibility indicates that the LNMO particles are much more complex structurally and may have anti-site defects or a second-phase with a different transition temperature. For a better understanding of the nature of the magnetic state and dynamic characteristics observed here for LNMO and LCMO nanoparticles, further detailed studies are needed.

REFERENCES

1. N. S. Rogado, J. Li, A. W. Sleight, and M. A. Subramanian, *Adv. Mater.*, 2005, **17**, 2225.
2. H. Guo, J. Burgess, S. Street, A. Gupta, T. G. Calvarese, and M. A. Subramanian, *Appl. Phys. Lett.*, 2006, **89**, 022509.
3. (a) M. Kitamura, I. Ohkubo, M. Kubota, Y. Matsumoto, H. Koinuma, and M. Oshima, *Appl. Phys. Lett.*, 2009, **94**, 132506; (b) J. Burgess, H. Guo, A. Gupta, and S. Street, *Vibr. Spectros.*, 2008, **48**, 113.
4. M. C. Sánchez, J. García, J. Blasco, G. Subías, and J. Perez-Cacho, *Phys. Rev. B*, 2002, **65**, 144409..
6. K. D. Truong, J. Laverdière, M. P. Singh, S. Jandl, and P. Fournier, *Phys. Rev. B*, 2007, **76**, 132413.
7. V. L. J. Joly, P. A. Joy, S. K. Date, and C. S. Gopinath, *Phys. Rev. B*, 2002, **65**, 184416.
8. Y. Q. Lin, and X. M. Chen, *J. Amer. Ceram. Soc.*, 2011, **94**, 782.
9. J. M. D. Coey, *Magnetism and Magnetic Materials*. Cambridge University Press: 2010.
10. I. Vrejoiu, M. Alexe, D. Hesse, and U. Gösele, *Adv. Funct. Mater.*, 2008, **18**, 3892.
11. Y. Mao, T.-J. Park, F. Zhang, H. Zhou, and S. S. Wong, *Small*, 2007, **3**, 1122.
12. Y. Mao, *RSC Adv.*, 2012, **2**, 12675.
13. I. G. Deac, J. F. Mitchell, and P. Schiffer, *Phys. Rev. B*, 2001, **63**, 172408.
14. M. Ziese, *J. Magn. Magn. Mater.*, 2008, **320**, 263.